Journal of Electrical and Computer Engineering Innovations
(JECEI)
Journal homepage: http://www.jecei.sru.ac.ir

Research paper

Optimization and Experimental Validation of an IPMSM for Electric Vehicles Targeting Torque Ripple Minimization, Average Torque and Efficiency Improvement

Alireza Shams [1], *Esmaeel Rokrok* [1,*], *Behrooz Rezaeealam* [1], *Abbas-Ali Zamani* [2]

[1] *Electrical Engineering Department, Lorestan University, Khorramabad, Iran.*

[2] *Department of Electrical Engineering, Technical and Vocational University (TVU), Tehran, Iran.*

Article Info

Article History:

Received 17 November 2025
Reviewed 05 January 2026
Revised 18 February 2026
Accepted 23 February 2026

Keywords:

Interior Permanent Magnet Synchronous Motor (IPMSM)
Electric Vehicle (EV)
Optimization of Motor Efficiency (OME)
Torque ripple reduction
Multi- Objective Particle Swarm Optimization (MOPSO)

[*]Corresponding Author's Email Address: *rokrok.e@lu.ac.ir*

Abstract

Background and Objectives: Interior permanent magnet synchronous machines (IPMSMs) have gained increasing attention in electric vehicle applications due to their high power density, desirable efficiency, and capability of delivering maximum torque over a wide speed range. Despite these advantages, challenges such as torque ripple and suboptimal efficiency remain. This study aims to propose a design and multi-objective optimization approach for the Stator-Optimized Delta-Type IPMSM (SO-DT-IPMSM) motor to enhance efficiency, reduce torque ripple, and improve average torque.

Methods: A multi-objective particle swarm optimization (MOPSO) was employed to determine the optimal set of stator parameters. In this study, an existing delta-type IPMSM rotor topology was adopted, and all rotor parameters were kept fixed, while the optimization was exclusively performed on stator geometry. Electromagnetic modeling and performance evaluation of the proposed design were carried out using Ansys Electronics. Following the optimization process, a prototype motor was manufactured and assembled based on the optimized design parameters, and experimental tests were conducted to validate the simulation results.

Results: Simulation results revealed significant improvements in the SO-DT-IPMSM compared with the Nissan Leaf IPMSM motor (Initial IPMSM). The optimized design achieved a 21% increase in average torque, 40% reduction in torque ripple, and 5% improvement in overall efficiency. Experimental tests performed on the fabricated prototype confirmed the accuracy of the simulation findings and demonstrated strong agreement between analytical and experimental data.

Conclusion: The proposed design and optimization approach effectively enhanced torque, torque ripple, and efficiency in the IPMSM. Beyond the validated experimental performance, the results demonstrate that the presented methodology can serve as a practical solution for improving electric vehicle motor performance. Moreover, the introduced optimization framework has the potential to be extended to other motor topologies and applications.

How to cite this paper:
A. Shams, E. Rokrok, B. Rezaeealam, A. Zamani, "Optimization and experimental validation of an ipmsm for electric vehicles targeting torque ripple minimization, average torque and efficiency improvement," J. Electr. Comput. Eng. Innovations, 14(2): 473-486, 2026.

DOI: 10.22061/jecei.2026.12722.906

URL: https://jecei.sru.ac.ir/article_2541.html

2345- 3044/© 2026 The Authors. Published by Shahid Rajaee Teacher Training University.

Introduction

In contemporary electric and hybrid vehicle drivetrains, PMSMs account for more than 80% of traction motor applications. This dominance is largely due to their ability to deliver high power density, maintain excellent efficiency across a wide speed range, and satisfy stringent vehicle performance requirements, as evidenced in vehicles such as the Nissan Leaf, Chevrolet Bolt, BYD E6, BMW i3, and Toyota Prius [1]-[3].

Although these motors possess high performance potential, their design faces numerous challenges. The stator structure and its geometric parameters directly impact average torque, torque ripple, core and copper losses, and ultimately, the motor's efficiency [4]. On one hand, reliance on rare-earth permanent magnets increases production costs and reduces supply chain stability [5]. On the other hand, phenomena such as torque ripple and acoustic vibrations affect performance quality and passenger comfort [6]. Alongside these issues, the simultaneous achievement of conflicting objectives such as increasing average torque, reducing torque ripple, and increasing efficiency turns the motor design problem into a complex multi-objective challenge [7]. Furthermore, traditional design methods based on trial-and-error or single-objective optimization lack sufficient capability to explore the large design space of the motor and find the precise balance point among performance objectives. Therefore, the need for an intelligent multi-objective optimization framework that can improve the electromagnetic performance, manufacturability, and overall efficiency of the motor is strongly felt. The design and optimization of IPMSMs have become a main research focus in recent years due to the growth of the electric vehicle industry. A significant portion of this research has focused on improving electromagnetic performance, reducing losses, and reducing torque ripple; however, many have overlooked the role of stator design as a key factor in systematic optimization.

Some research groups have focused on optimizing rotor topology, including V-shaped, inverted-V, asymmetric structures, and magnetic flux path optimization. These studies have managed to increase average torque and reduce torque ripple but have largely neglected the effect of stator shaping and its manufacturing constraints [8]-[11]. Additionally, many of the proposed methods require heavy finite element analysis (FEA) analyses and are not very cost-effective for industrial applications. Other studies have used multi-objective approaches such as evolutionary algorithms, surrogate models based on machine learning, and multilevel methods to explore the extensive IPMSM design space. These methods have often achieved significant accomplishments in reducing computational cost and increasing prediction accuracy [12]-[17]. However, many of these studies face challenges such as reduced population diversity, premature convergence, or excessive algorithm complexity, which limit industrial implementation. Studies related to stator shaping have been less frequent and often only address components such as tooth shape, slot opening, and bridge dimensions. Some of this research has shown that stator design directly impacts average torque, core losses, and torque ripple, and in many cases, its influence is greater than that of rotor design [18]-[20]. However, most of these works have been either single-objective or have ignored manufacturing constraints such as minimum tooth thickness, producible slot depth, and local core saturation. In much of the previous research, although significant improvements in the design and optimization of IPMSMs have been achieved, a fundamental gap remains: None of these studies has provided a simple, industrially viable, yet multi-objective design framework for optimizing stator parameters; a framework that can systematically and simultaneously guarantee three key criteria: increasing average torque, reducing torque ripple, and improving efficiency. Most existing research has focused only on a limited part of the geometry or has not considered the real constraints of stator manufacturing and producibility. Furthermore, some of the optimization methods used face problems such as reduced population diversity and insufficient Pareto front coverage, which can lead to suboptimal solutions. Therefore, the need for a more accurate, practical, and industry-applicable method is still strongly felt; a need that the present research seeks to address.

To this end, this study presents a stator design and optimization method for an SO-DT-IPMSM intended for electric vehicle applications, based on an MOPSO algorithm. An existing delta-type IPMSM rotor topology is adopted as the baseline and kept unchanged throughout the optimization process, allowing the influence of stator design to be isolated and systematically evaluated. In the proposed approach, key stator design parameters, including tooth width, slot depth, air gap length, slot opening width, slot opening height, and stator yoke, are selected through an importance analysis of design parameters, supported by analytical formulations and electromagnetic principles, to identify the most influential variables in IPMSM optimization. The optimization problem is then formulated in a multi-objective manner and solved using FEA, where three primary objectives—maximization of average torque, reduction of torque ripple, and improvement of efficiency are pursued simultaneously. By focusing exclusively on stator design while keeping all rotor parameters constant, the proposed framework

reduces design complexity and enhances industrial feasibility, particularly for upgrading existing motor platforms. The results demonstrate that the proposed method achieves superior electromagnetic performance compared to conventional optimization approaches, providing an effective and practical pathway for the development of next-generation IPMSMs for electric vehicle traction systems.

The article is structured such that Section 2 elaborates on the analytical model and introduces the base IPMSM motor.

In Section 3, the MOPSO algorithm is first introduced. Subsequently, the definitions and importance analysis of the variables, the selection of optimization objectives, and the execution of the MOPSO algorithm are described.

Section 4 presents the simulation results based on Finite Element Analysis and compares the performance of the optimized SO-DT-IPMSM with the initial IPMSM.

Then, in Section 5, the simulation data are first experimentally validated with a prototype of the optimized SO-DT-IPMSM, and its experimental results are then compared with the experimental results of the Initial IPMSM.

Finally, Section 6 summarizes the findings and provides suggestions for future research directions.

IPMSM Motor Topology

The objective of this study is to improve the performance of an 80 kW IPMSM from the Nissan Leaf electric vehicle [23] with a rated speed of 2100 rpm. Compared to the Surface-mounted Permanent Magnet Synchronous Motor (SPMSM) type, in the IPMSM, the magnets are embedded inside the rotor. This feature eliminates the risk of magnet detachment at high speeds due to centrifugal force. Furthermore, the IPMSM can increase the motor's power density through the reluctance torque generated by the magnetic circuit's asymmetry. This research employs a single-layer, distributed, full-pitch winding in the stator. By distributing the coils of each phase across several adjacent slots, this winding enhances the main component of the Magneto Motive Force (MMF) and reduces mechanical harmonics. This structure results in a more sinusoidal flux, reduced cogging torque, lower noise, and reduced core losses; although its winding factor and slot space utilization are lower compared to double-layer or concentrated windings. The IPMSM under investigation features a rotor with a delta-shaped structure, 8 poles, and a stator with 48 slots. The delta-shaped rotor structure provides higher output torque and better performance in the field-weakening region, which is why it is widely used in high-speed electric vehicle motors. The topology of the IPMSM studied in this paper is shown in Fig. 1.

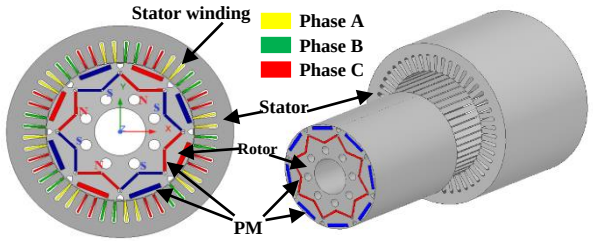

(b) (a)

Fig. 1: a) Exploded view of the studied IPMSM motor. b) Schematic diagram of the studied IPMSM motor

The parameters of the initial design specifications for the studied IPMSM are as shown in the Table 1.

Table 1: The parameters of the initial design specifications for the studied IPMSM

Type of Motor	SO-DT-IPMSM
Number of stator slot/rotor pole	48/8
Output power (kw)	80
Rated speed (r/min)	2100
Rated torque (N.m)	280.7
Efficiency (%)	92.5
Rated current (A)	340

Proposed Optimal Design Procedure for SO-DT-IPMSM

A. Principle of Particle Swarm Optimization

Particle Swarm Optimization (PSO) is a heuristic intelligent optimization algorithm developed by Kennedy and Eberhart [24]. Inspired by the foraging behavior of birds, PSO searches for optimal solutions through information sharing and cooperation among individuals. Initially, the algorithm randomly generates a set of initial solutions and then iteratively searches for the global optimum. In each iteration, the next search direction is determined based on the global best solution and the individual's best solution from the previous iteration. Due to its simple structure and strong search capabilities, this algorithm has been widely used in parameter identification and maximum power point tracking [25]. This algorithm primarily consists of five steps: Initialization, Velocity Update, Position Calculation, Revision of Individual Best Solutions, and Update of the Global Best Solution.

1) Initialization

A set of N particles is randomly generated with initial positions and velocities. The fitness of each particle is then evaluated using the fitness function f(x).

2) Velocity Update

The velocity of each particle is updated according to:

$$v_i = \omega \times v_i + c_1 \times rand() \times (Pb^i - x_i) + c_2 \times rand() \times (Pg(k) - x_i) \quad (1)$$

where, ω (0 ≤ ω ≤ 1) denotes the inertia weight, c_1 and c_2 are learning coefficients, v_i and x_i are the velocity and position of particle i, rand() is a uniformly distributed random number in [0,1], Pb^i is the personal best position of particle i, and Pg(k) is the global best position of the swarm at iteration k.

3) Position Update

After updating the velocities, the position of each particle is recalculated as:

$$x_i = x_i + v_i \quad (2)$$

This equation ensures that each particle moves according to its newly computed velocity.

4) Update of Individual Best Positions Each particle's personal best position is updated according to:

$$Pb^i(k+1) = \begin{cases} Pb^i(k) & f[Pb^i(k+1)] \geq f[Pb^i(k)] \\ Pb^i(k+1) & f[Pb^i(k+1)] < f[Pb^i(k)] \end{cases} \quad (3)$$

This step ensures that a particle's personal best position reflects the best fitness it has achieved so far.

5) Update of the Global Best Position

The global best position of the swarm is determined as:

$$Pg(k) = \arg\min f[Pb^i(k)] \qquad 1 \leq i \leq N \quad (4)$$

where, N is the total number of particles. The global best position corresponds to the personal best position yielding the minimum objective function value among all particles.

During each iteration, particles update their velocities and positions using (1) and (2). Subsequently, each particle updates its personal best according to (3). Once all personal bests are revised, the global best is updated according to (4).

This process is repeated until the termination criterion is satisfied.

Finally, the algorithm halts and outputs the optimized solution.

B. The Flowchart of Optimal Design Procedure for SO-DT-IPMSM

Fig. 2 illustrates the flowchart of the proposed multi-objective optimization method for the initial IPMSM, whose main steps are outlined below:

Step 1: Create Initial Model and Perform Preliminary Analysis.

An initial model of the Initial IPMSM is created in Ansys Electronics software. A preliminary electromagnetic analysis is performed on the model to evaluate the motor's baseline behavior in terms of magnetic field, torque, losses, and other key parameters. Performance graphs are extracted for result comparison.

Step 2: Select Design Variables.

In this step, design variables affecting the motor's geometric or electromagnetic parameters are first introduced. Then, through an analysis of various references, the most critical design variables used for optimizing the Initial IPMSM are selected. Subsequently, based on the selected design variables, various references, and the structure of the studied motor, the design constraints are chosen.

Step 3: Initialize MOPSO Algorithm Parameters.

In this step, the key parameters of the algorithm, such as population size, maximum iterations, inertia weight, learning coefficients (c_1, c_2), and velocity limits, are initialized according to the specific requirements of the optimization problem.

Step 4: Evaluate Samples in Ansys Electronics.

Each design vector is imported into Ansys Electronics software, and an electromagnetic simulation is performed. The optimization objectives are calculated and extracted for each sample.

Step 5: Check Stopping Criterion.

It is checked whether the maximum allowed number of algorithm iterations has been reached. If not, the MOPSO algorithm is updated, and new design vectors are generated (return to Step 3). If yes, the optimization process ends.

Step 6: Select Optimal Design.

Optimal designs are extracted from the generated Pareto Front by the MOPSO algorithm. Based on the Design Strategy, one or more final designs are selected.

Step 7: Fabricate the Proposed Optimized SO-DT-IPMSM.

The final step of the design method involves fabricating a physical prototype of the SO-DT-IPMSM, built according to the optimized design parameters, provided the simulation results satisfactorily meet the pre-defined performance criteria.

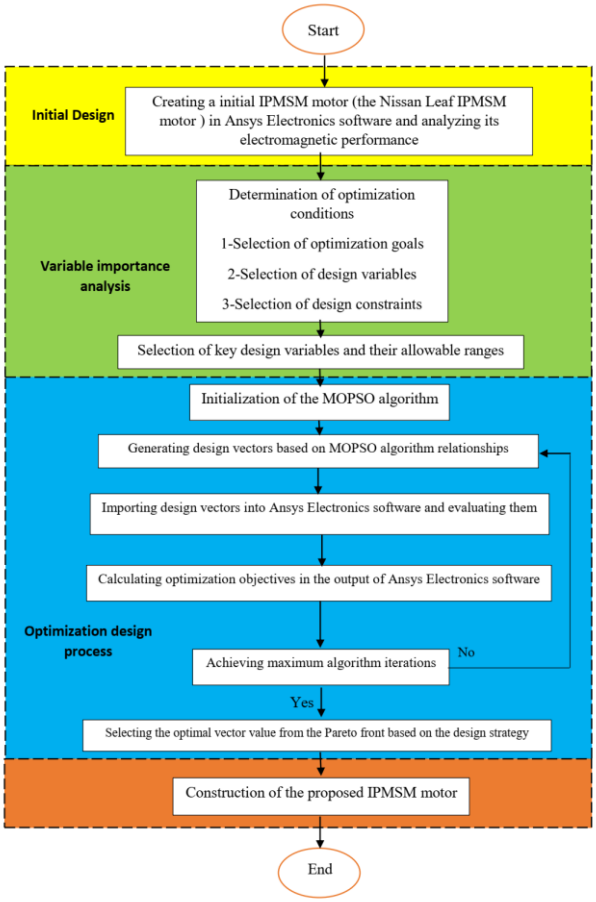

Fig. 2: Multi-objective optimization flowchart for IPMSM motor.

Selection of Design Variable

Fig. 3 shows the parametric FEA model of the SO-DT-IPMSM created in Ansys Maxwell software, which includes 22 design parameters.

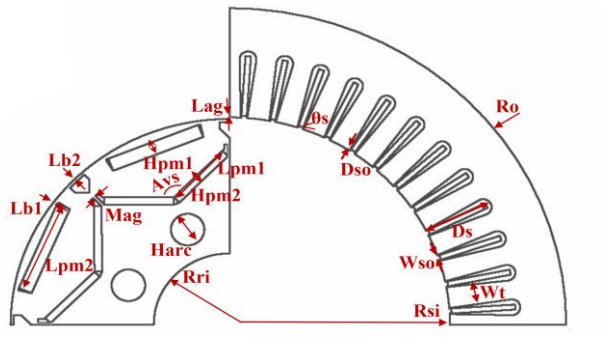

Fig. 3: SO-DT-IPMSM parametric model.

Based on references [26]-[36], it is not necessary to optimize all 22 design parameters, as some of them can be predetermined during the initial design stage. The inner stator radius (R_{si}) is defined according to the rated power, power factor, efficiency, and nominal speed, whereas the outer stator radius (R_o) is constrained by the installation space available for the IPMSM in electric vehicles. Since the optimization process is focused solely on the stator, the rotor parameters are kept fixed and are adopted from the Initial IPMSM as reported in reference [23]. The symbols of the structural parameters of the studied IPMSM are labeled in Fig. 3, and their corresponding values are listed in Table 2.

Table 2: Values of structural parameters of the studied IPMSM

Categories	Parameters	Symbol	Unit	Value
Stator parameters	Inner radius of stator	Rsi	mm	65.5
	Outer radius of stator	Ro	mm	100
	Slot opening width	Wso	mm	2
	Inner slot width	Bs1	mm	2
	Outer slot width	Bs2	mm	5
	Slot opening height	Dso	mm	0.5
	Slot neck depth	Hs1	mm	0
	Slot depth	Ds	mm	18
	Tooth width	Wt	mm	5.4
	Stator yoke	Wy	mm	13.25
	Air gap length	Lag	mm	1
	Tooth tip angle	Θs	deg	30
Rotor parameters	Inner radius of rotor	Rri	mm	22.5
	V-shaped PMs length	Lpm1	mm	30
	Straight-shaped PMs length	Lpm2	mm	40
	V-shaped PMs clamp angle	Avs	deg	130
	External Magnetic Bridge Width Straight Shape	Lb1	mm	1.3
	Flux barrier	Lb2	mm	1.6
	Internal Magnetic Bridge Width	Mag	mm	1.27
	Straight-shaped PMs width	Hpm1	mm	4
	V-shaped PMs width	Hpm2	mm	2
	Diameter of Rotor hole	Harc	mm	10

The materials and design dimensions, including the rotor core and permanent magnets, are considered fixed in this design. The only difference lies in the distinct dimensions and structure of the stator core slots and teeth, which are considered in the proposed design.

Importance Analysis of Design Parameters Effective in IPMSM Optimization

In order to define the motor's performance objectives and determine the optimizable variables, the electromagnetic relationships related to efficiency, torque, and flux behavior were first examined. Recent studies on IPMSM design for electric vehicles identify high efficiency, stable average torque, low torque ripple, and robust dynamic behavior as key performance indicators. Studies conducted in recent years show that these characteristics are directly influenced by the geometry of the flux paths and the field distribution in the stator section.

Motor efficiency, which is one of the main objectives of the optimization process in this research, can be calculated from the following equation:

$$\eta = P_e / (P_e + P_{loss}) = T_e.\omega / (T_e.\omega + P_{loss}) \quad (5)$$

where, T_e is the electromagnetic torque, ω is the angular speed, and P_{loss} includes the sum of copper, iron, mechanical, and stray losses. According to this relationship, any change in geometry that affects torque generation or the amount of losses will directly impact the final efficiency.

By reviewing 11 reference papers [26]-[36] in the field of sensitivity analysis and optimization of IPMSM, six geometric parameters of the stator that show high sensitivity to torque and losses have been selected. These parameters include tooth width, slot depth, air gap length, slot opening width, slot opening height, and stator yoke thickness.

The selection of this set was based on two criteria:

1) Direct relevance to the flux behavior in the air gap and tooth region,

2) A determining role in controlling torque ripple and preventing core saturation.

Tooth width is a key factor in determining torque due to its effect on the flux passing through the tooth and, consequently, the linked flux. The torque in an IPMSM is defined by the following equation:

$$T_e = (3/2).p.(\phi_f.i_q + (L_d - L_q).i_d.i_q) \quad (6)$$

where, T_e is the electromagnetic torque, p is the number of pole pairs, and i_d, i_q, L_d, L_q, and ϕ_f are the d-q axis currents, inductances, and PM flux linkage, respectively.

Slot depth represents the effective volume for winding, and its changes directly affect the resistance and copper losses. This behavior is described by the relations:

$$R = \rho.l / A_{slot} \quad , \quad P_{cu} = R.I^2 \quad (7)$$

where, R is the winding resistance, ρ denotes the electrical resistivity of the conductor material (copper), l is the effective length of the conductor, and A_{slot} represents the effective slot cross-sectional area available for the winding. In addition, P_{cu} denotes the copper losses, and I is the current flowing through the winding. According to (7), increasing the effective slot area—resulting from an increase in slot depth leads to a reduction in the winding resistance and, consequently, a decrease in copper losses. Therefore, slot depth is a key geometric parameter that significantly influences the loss characteristics and overall efficiency of the electrical machine.

The air-gap flux φ is approximately inversely proportional to the air-gap length g. This relationship can be expressed as

$$\phi \ \alpha \ 1/g \quad (8)$$

The air-gap length simultaneously affects torque, torque ripple, and efficiency, since an increase in g reduces the air-gap flux, leading to a lower electromagnetic torque, whereas a smaller g increases flux but may exacerbate torque ripple and core losses.

The geometric parameters of the stator slot opening, namely the slot opening width and slot opening height, play an important role in determining the electromagnetic performance of the IPMSM. These parameters directly affect the magnetic field distribution in the air-gap region and the amount of leakage flux, thereby influencing torque quality and loss characteristics.

Torque ripple in IPMSMs originates from periodic variations in the magnetic co-energy as a function of rotor position. Accordingly, the impact of slot opening geometry on torque behavior can be expressed by

$$T(\theta) = dWmag / d\theta \quad (9)$$

where, W_{mag} is the magnetic co-energy stored in the machine. The slot opening dimensions alter the effective air-gap permeance distribution, thereby modulating $W_{mag}(\theta)$ and its derivative, which directly determines the torque profile. Increased slot width or height typically enhances leakage flux and introduces higher spatial harmonics in the air-gap field, leading to more pronounced torque ripple. Therefore, careful optimization of slot width and height is essential for minimizing torque ripple while maintaining acceptable levels of stator saturation and manufacturing feasibility.

Finally, the yoke thickness h_{yoke} plays a critical role in providing a low-reluctance return path for the magnetic flux. An insufficient yoke thickness leads to increased flux density in the yoke region, which in turn raises core losses due to saturation effects. This relationship can be expressed as:

$$B_{yoke} = \phi / A_{yoke} \quad (10)$$

where, ϕ is the magnetic flux per pole and A_{yoke} is the yoke cross-sectional area. Since A_{yoke} is directly proportional to the yoke thickness h_{yoke}, a reduction in h_{yoke} results in an increased yoke flux density B_{yoke}. Elevated flux density intensifies core losses and may lead to local magnetic saturation, thereby degrading machine performance. Therefore, the stator yoke thickness must be carefully selected to maintain the flux density below the saturation limit while minimizing material usage.

These key parameters significantly influence the optimization objectives and are therefore selected as design variables in the multi-objective model.

Their corresponding variation ranges are provided in Table 3.

Table 3: Range of variation of key parameters of the IPMSM stator under study

Parameters	Symbol	Unit	Initial	Range
Tooth width	Wt	mm	5.4	3.5-6.5
Slot depth	Ds	mm	18	17-27
Air gap length	Lag	mm	1	0.5-1
Slot opening width	Wso	mm	2	1.5-2.5
Slot opening depth	Dso	mm	0.5	0.5-1
Stator yoke	Wy	mm	10	3-15

The range of values for the design variables must adhere to the following optimization constraints:

(1) The slot fill factor represents the proportion of copper occupying the slot area. Since coil insertion is usually carried out by automated manufacturing processes, this factor should generally not exceed 75%. At the same time, an excessively low fill factor is undesirable, as insufficient copper packing may cause wire movement during operation and increase the risk of insulation wear. Considering these aspects, the slot fill factor in this study is constrained within the following limits:

$$60\ \% \le S_f \le 75\ \% \quad (11)$$

(2) To prevent excessive saturation of the motor's average flux density, which degrades IPMSM performance, the constraints for the average flux density in the stator tooth section (B_t) and the average flux density in the stator yoke section (B_j) must be as follows:

$$B_t \le B_{sat} \quad and \quad B_j \le B_{sat} \quad (12)$$

where, B_{sat} is the saturation flux density of the silicon steel sheet. In this paper B_{sat} is 1.95 T.

To prevent an excessive temperature rise during motor operation, which could lead to the demagnetization of the permanent magnets, the current density (J) constraints must be defined as [31]:

$$J \le 10 A.mm^{-2} \quad (13)$$

Selection of Optimization Objectives

Electric vehicles encounter a wide range of dynamic driving conditions, requiring the IPMSM to deliver sufficiently high torque for frequent events such as startup, acceleration, braking, and hill climbing. To maintain smooth and stable operation, the torque ripple of the IPMSM must also be minimized. In addition, achieving a long driving range in EVs demands that the motor operates with low losses and high efficiency. Considering the strong interdependence between losses and efficiency, this study focuses on optimizing the IPMSM's average torque (T_a), torque ripple (T_r), and efficiency (η) as the primary performance targets. The average torque Ta is defined as follows:

$$T_a = avg \quad (T_e) \quad (14)$$

T_r is defined as follows:

$$T_r = (T_{em\_max} - T_{em\_min}) / (T_a) \quad (15)$$

where, T_{em_max} and T_{em_min} are the maximum and minimum electromagnetic torques, respectively. As the stator winding is already determined based on the voltage requirements of the power source, it does not need to be modified during the optimization process. Consequently, copper losses remain essentially constant. Therefore, in calculating the total losses, only the core losses and permanent magnet losses are taken into account. The total loss P_t is defined as follows:

$$P_t = P_{ironcore} + P_{pm} \quad (16)$$

where, $P_{ironcore}$ and P_{pm} are the core losses and PM losses, respectively.

Although the efficiency η has been introduced earlier in the importance analysis, it is redefined here in the context of optimization objectives, linking it directly to total losses for clarity in the optimization process. Subsequently, the motor efficiency is defined as follows:

$$\eta = (T_a.\omega) / (T_a.\omega + P_t) \quad (17)$$

where, ω is the angular speed of the electric motor, T_a is the average torque, and P_t is the total loss.

This study focuses on optimizing output torque, minimizing torque ripple, and increasing motor efficiency

as the primary objectives. Given that our goal is to improve the performance of the Initial IPMSM, the rated values of this motor output torque of 280 N.m, torque ripple of 10.65%, and efficiency of 92.5% have been used in the objective function below. Therefore, the optimization objectives for the SO-DT-IPMSM are expressed in the following equation.

$$\min \begin{cases} f_1(x) = c_1 \dfrac{280}{T_a} \\ f_2(x) = c_2 \dfrac{92.5}{\eta} \\ f_3(x) = c_2 \dfrac{T_r}{10.65} \end{cases} \tag{18}$$

where, x is the optimization variable (stator parameters), and the value range of the optimization variables is shown in Table 3. c_1 and c_2 are the weighting coefficients for the optimization objectives. Since the IPMSM is used in an electric vehicle, the optimization of motor efficiency is more critical in this research; therefore, the weighting coefficients are chosen as c_1=0.3 and c_2=0.7. The Pareto solution set is obtained according to the algorithm settings and the methods described above, as shown in Fig. 4(a) and Fig. 4(b).

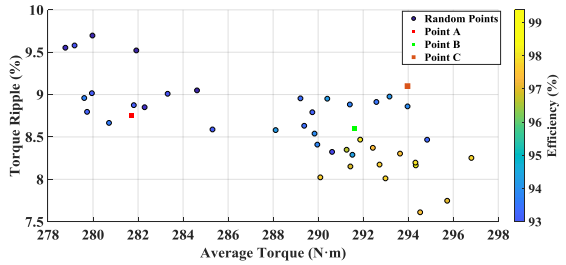

(a)

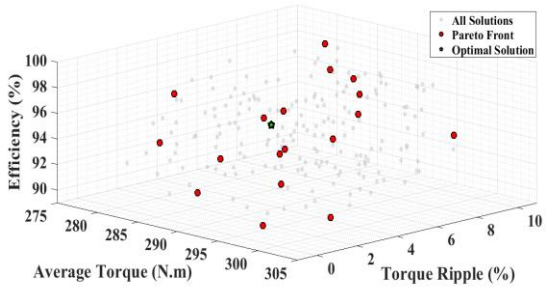

(b)

Fig. 4: a) 3D Pareto front diagram of the MOPSO optimization algorithm a) 3D diagram b) 2D diagram with three optimal points.

It can be observed that the optimization objectives $f_1(x)$, $f_2(x)$, and $f_3(x)$ cannot all achieve their optimal values simultaneously. To establish a reasonable compromise among the three optimization objectives, three candidate points—A, B, and C—are selected from the chart for comparison based on the order of average torque. Next, the FEA method is employed to determine the average torque, torque ripple, and efficiency of the motor at these three operating points, and the results are summarized in Table 4.

Table 4: Comparison of optimization goals at three points A, B, and C and the output of the Initial IPMSM

Candidate solutions	MOPSO+ FEA results		
	T_a(N.m)	T_r(%)	η(%)
A	281.7	8.7	96.3
B	291.6	8.6	95.8
C	293.97	9.2	97.22
Initial IPMSM	280.7	15.16	92.5

This paper presents a multi-objective optimization framework for the design of an electric vehicle traction motor, which combines MOPSO with FEA using Ansys Electronics. As presented in Table 4, among the three evaluated solutions, Candidate C demonstrates the highest average torque Ta and efficiency η, while exhibiting the lowest torque ripple T_r relative to Candidates A and B.

Accordingly, Candidate C is chosen as the optimal configuration for the stator parameters in this study. In the context of electric vehicle operation, where high efficiency extends driving range, sufficient torque ensures strong acceleration, and minimal torque ripple improves NVH performance, Candidate C represents the most favorable design alternative. Table 5 shows the optimization results for the SO-DT-IPMSM.

Table 5: Comparison of SO-DT-IPMSM optimization results

	Parameters	Unit	Initial Value	MOPSO+ FEA results
Optimization Parameters in stator of IPMSM	W_{so}	mm	2	1.88
	D_{so}	mm	0.5	1
	D_s	mm	18	17.9
	L_{ag}	mm	1	1
	W_t	mm	5.4	5.5
	W_y	mm	10	13.4
Optimization objectives	T_a	N.m	280.7	293.97
	T_r	%	10.65	9.2
	η	%	92.5	97.22

Optimization Result Discussion

The optimization results indicate that the stator geometric parameters play a critical role in shaping the

electromagnetic performance of the SO-DT-IPMSM. Among the ways examined, it specifies the length of the air gap which indicates that on the electromagnetic between the rotor and the stator. Reducing the air gap increases the magnetic flux density and thus the average torque. However, if it is reduced too much, it will lead to local saturation and increase the torque ripple. In particular, the slot opening width and height significantly influence the air-gap flux distribution and cogging torque characteristics.

By optimizing the slot opening dimensions, the spatial harmonics of the air-gap flux density are effectively suppressed, leading to a noticeable reduction in torque ripple. A narrower and well-proportioned slot opening improves flux continuity across the air gap, thereby reducing localized flux concentration and electromagnetic force fluctuations.

The stator tooth width directly affects magnetic saturation and harmonic content in the stator core. Increasing the effective tooth width reduces local saturation and improves flux-carrying capability, which contributes to smoother flux distribution and lower harmonic distortion in the stator magnetic field. This improvement is particularly evident in the reduction of torque ripple components and enhanced efficiency under load. Furthermore, the optimized overall stator geometry, including yoke thickness and slot depth, increases torque density by enabling higher effective air-gap flux and improved magnetic utilization of the stator core. These combined geometric improvements enhance average torque output while maintaining acceptable core losses, demonstrating that stator-focused optimization is a highly effective approach for improving IPMSM performance.

Electromagnetic Performance Comparison

To assess the effectiveness of the proposed methodology, a detailed comparison of the electromagnetic performance was performed between the standard Initial IPMSM [23] and the optimized SO-DT-IPMSM using FEA.

The comparison focuses on the three main objectives of this study: increasing average torque, reducing torque ripple, and improving efficiency. Figures 5 and 6 summarize the results.

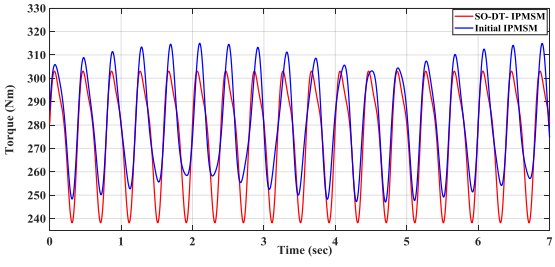

(a)

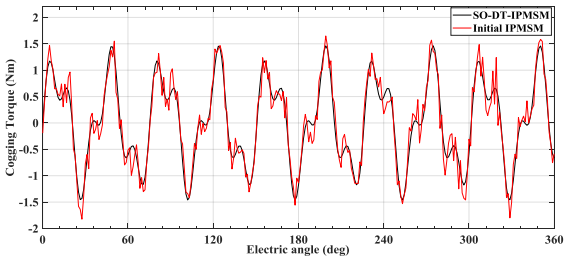

(b)

Fig. 5: Comparison of electromagnetic performance a) Electromagnetic torque of Initial IPMSM and SO-DT-IPMSM. b) Their cogging torque.

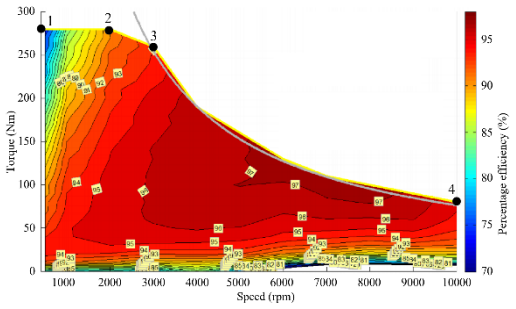

(a)

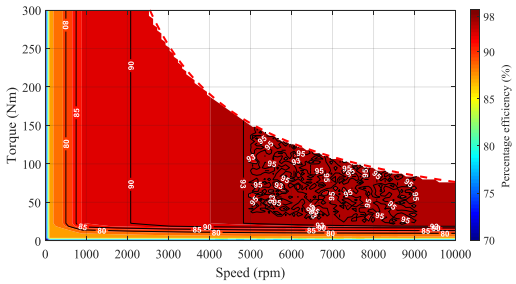

(b)

Fig. 6: Comparison of efficiency distribution of a) Initial IPMSM reference [23]. b) SO-DT-IPMSM.

Average Torque Improvement

As shown in Fig. 5, the optimized SO-DT-IPMSM produces 21% higher average torque compared to the initial design. This improvement is primarily attributed to the systematic optimization of key stator parameters, including tooth width and stator geometry, which enhance torque density. The stepwise analysis confirms that each selected stator parameter contributes directly to the overall torque improvement. These results demonstrate that the proposed optimization method effectively increases the motor's torque output without altering rotor parameters, thereby maintaining design simplicity and industrial viability.

Torque Ripple Reduction

In addition to average torque, torque ripple is significantly reduced by 40% in the optimized motor. The reduction in torque ripple is mainly due to the careful

optimization of slot opening width, which smooths the magnetic flux distribution and minimizes harmonic distortions. This improvement ensures better motor stability, reduced acoustic vibration, and improved passenger comfort, particularly under variable load conditions. Furthermore, as can be observed from Fig. 4(b), the maximum cogging torque is reduced from 1.4 N·m to 1.12 N·m, indicating a 20% reduction. These three factors have significantly improved the motor stability. The reported values were calculated according (6), (9), and (14).

Efficiency Enhancement

Fig. 6 presents the efficiency distribution of both the initial and optimized motors. The SO-DT-IPMSM exhibits a wider operating range with efficiency exceeding 92.5%, compared to the initial design. At rated speed, efficiency rises from 92.5% to approximately 97%, while above rated speed, it reaches nearly 98%. This improvement is directly attributed to reduced core and copper losses, resulting from the optimized stator geometry and minimized torque ripple. These results demonstrate that the proposed stator optimization method effectively enhances both electromagnetic performance and overall energy conversion efficiency.

Overall, the sequential analysis confirms that the proposed multi-objective optimization effectively achieves the study's objectives: enhancing average torque, reducing torque ripple, and improving efficiency. The stepwise evaluation also clarifies how specific stator parameters contribute to each performance metric, making the methodology transparent and reproducible.

Results and Discussion

This section presents the experimental validation of the proposed SO-DT-IPMSM. A prototype was fabricated and tested under various load conditions to evaluate average torque, torque ripple, current harmonics, and efficiency, to verify the accuracy of the FEA simulations and confirm the practical effectiveness of the optimized design.

Fabrication of the Proposed SO-DT-IPMSM and Experimental Validation of Results

To validate the simulation results, the SO-DT-IPMSM with a 48-slot/8-pole configuration was fabricated and tested, as shown in Fig. 7.

The drive system uses an FPGA-based Kintex 7 controller implementing Field-Oriented Control (FOC). The rotor position is measured using an Autonics EP50S8-1024-2F-P-24 absolute encoder, which ensures accurate rotor angle measurement even after power loss. Phase currents were measured using an LA 200-P current sensor (range 0–±300 A, bandwidth 0–100 kHz), and the DC-link voltage was set at 400 V with a rated current of 340 A and a switching frequency of 10 kHz. Measurement accuracy and sensor resolution were carefully considered to ensure reliable results.

(a)

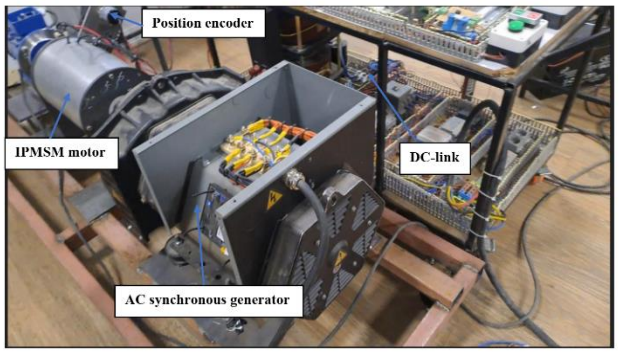

(b)

Fig. 7: Testing on SO-DT-IPMSM a) Rotor and stator configuration, b) Laboratory test setup.

During testing, the motor was evaluated under both no-load and variable-load conditions. Variable-load operation was achieved by mechanically coupling a three-phase synchronous generator to the motor shaft and applying an adjustable resistive load at the generator output. This setup allowed precise control of load torque, enabling both constant and variable load profiles representative of electric vehicle traction applications. All measurements were conducted under steady-state and constant-speed conditions, with torque characteristics evaluated at predefined load levels.

Average Torque and BEMF Analysis

Fig. 8 compares the phase BEMF of the initial IPMSM and the SO-DT-IPMSM. The optimized stator design (tooth shape, slot width, and stator yoke) reduces higher-order harmonics, resulting in a waveform closer to a sinusoid. This reduction in BEMF harmonics directly improves torque output and reduces ripple.

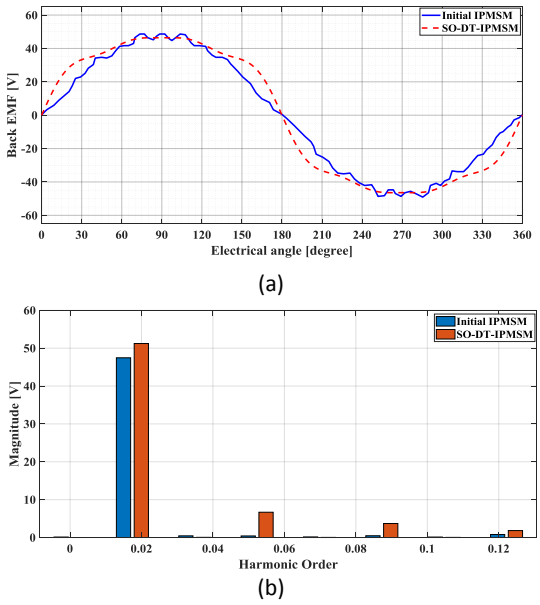

Fig. 8: a) BEMF and harmonic analysis of the initial IPMSM motor b) SO-DT-IPMSM.

Fig. 9 shows that the optimized SO-DT-IPMSM generates 21% higher average torque than the initial IPMSM.

This improvement is primarily due to the systematic optimization of key stator parameters, including tooth width and stator shape, which enhance torque density. Stepwise analysis confirms that each selected stator parameter contributes directly to the overall torque increase. These results demonstrate that the proposed optimization method effectively enhances torque output without altering rotor parameters, maintaining simplicity and industrial viability.

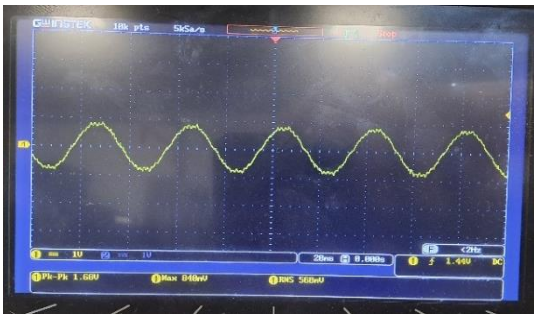

Fig. 9: Experimental BEMF waveform of the SO-DT-IPMSM.

Torque Ripple and Current Harmonics

Fig. 10 shows the phase current waveforms under rated load. The SO-DT-IPMSM exhibits nearly sinusoidal currents with significantly reduced harmonic distortion.

- The phase current Total Harmonic Distortion (THD) decreased from 11.2% (initial IPMSM) to 3.1% after optimization.
- The current ripple decreased from 4.5% to 2.8% of RMS value.
- The reduction in torque ripple is approximately 40%, as a result of improved air-gap flux distribution and reduced BEMF harmonics.

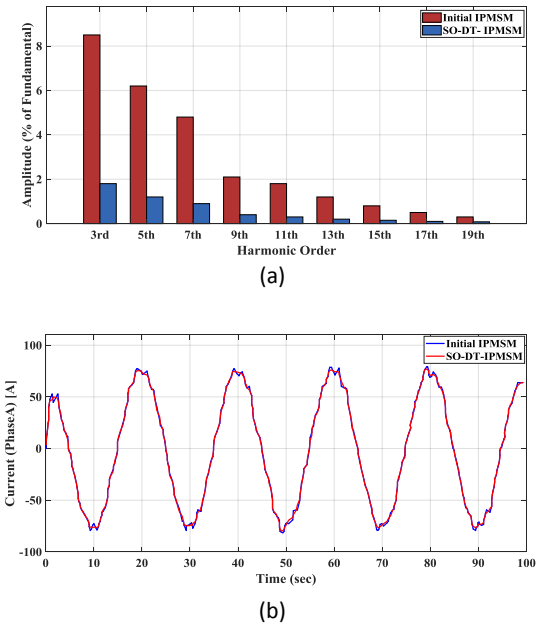

Fig. 10: a) Phase current and harmonic analysis of the initial IPMSM motor b) SO-DT-IPMSM.

These improvements are directly related to the optimized stator slot geometry and flux path, which minimize harmonics and smooth torque production, resulting in lower acoustic noise, smoother motor operation, and higher efficiency.

Efficiency Improvement

The experimental results also confirm the enhanced efficiency of the optimized SO-DT-IPMSM. Reduction in current harmonics and torque ripple decreases both copper and core losses, aligning with simulation predictions. Table 6 summarizes the comparison between the initial IPMSM and the optimized motor, showing significant improvements in torque, torque ripple, and efficiency across all tested load conditions.

Table 6: Comparison results optimization of SO-DT-IPMSM and Initial IPMSM

Experimental results of Initial IPMSM			Experimental results of SO-DT-IPMSM		
T_a (N.m)	T_r (%)	η(%)	T_a (N.m)	T_r (%)	η(%)
280.70	15.16	92.50	293	9	97

Overall, the experimental validation demonstrates that the proposed multi-objective stator optimization:

1. Increases average torque through improved stator design.
2. Reduces torque ripple and current harmonics, enhancing motor stability and reducing noise.

Improves efficiency by minimizing losses in the stator and rotor. The results confirm the accuracy of the FEA simulations and validate the effectiveness of the SO-DT-IPMSM design methodology under practical operating conditions. The sequential presentation ensures that each objective is clearly linked to specific design changes and measurable improvements. Fig. 11 shows the measured phase current waveform of the actual SO-DT-IPMSM under rated load conditions.

As can be observed, after optimization, the current waveform has become nearly sinusoidal and its harmonic distortion has been significantly reduced. The phase current THD decreased from approximately 11.2% in the initial model to about 3.1% after optimization. Furthermore, the current ripple was reduced from 4.5% of the RMS value to approximately 2.8%. This improvement is due to the modification of the stator slot geometry and the optimization of the flux distribution in the air gap, which led to a reduction in the harmonic components of the BEMF. Consequently, the output torque ripple has also been reduced by approximately 40%, resulting in smoother motor operation, lower noise, and higher efficiency.

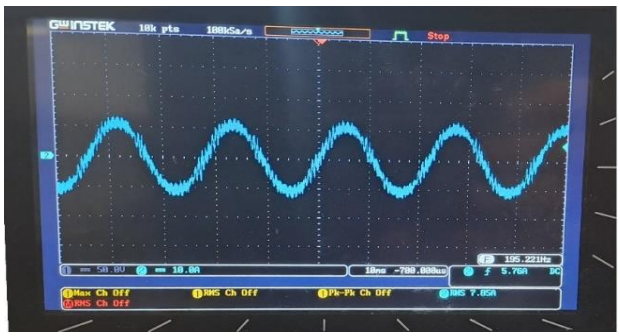

Fig. 11: Experimental phase current waveform of the SO-DT-IPMSM under rated load conditions.

Conclusion

This paper presented a novel SO-DT-IPMSM structure and benchmarked its performance against the Initial IPMSM of the Nissan Leaf EV due to their structural similarities. By employing an optimized stator design including slot and tooth shape refinement and key parameter optimization, the proposed method effectively reduced flux leakage and established a more favorable magnetic field distribution, resulting in increased torque density and improved overall motor efficiency. Comparative analysis demonstrated that the SO-DT-IPMSM delivers superior performance, achieving a torque of 293.7 Nm, a reduced torque ripple of 9.07%, and an efficiency of 97.22%, significantly outperforming the 92.5% efficiency of the Initial IPMSM motor. A prototype of the SO-DT-IPMSM was also manufactured and tested, validating the simulation results. Furthermore, a multi-objective optimization algorithm based on MOPSO was introduced to obtain a high-performance IPMSM characterized by high torque, high efficiency, and low torque ripple for EV applications. The results confirm that the proposed optimization framework can effectively enhance the overall performance of the reference IPMSM while reducing computational time compared to traditional FEA-based optimization procedures, without compromising accuracy.

Future work will focus on extending the optimization framework to include both stator and rotor parameters as well as broader performance objectives. Moreover, motor control investigations for the developed prototype will be conducted to further validate and demonstrate the effectiveness of the proposed optimization approach.

Author Contributions

A. R. Shams performed the simulations, analyzed the results, contributed to the development and commissioning of the optimized motor, and drafted the initial version of the manuscript. Dr. E. Rokrok supervised the research process, performed the simulations, validated the results, and conducted the final review of the manuscript. Dr. A.A. Zamani supervised the research process, performed the simulations, validated the results, and contributed to the editing and final revision of the manuscript. Dr. B. Rezaeealam supervised the research process of the work, validated the results.

Conflict of Interest

The authors declare no potential conflict of interest regarding the publication of this work. In addition, the ethical issues including plagiarism, informed consent, misconduct, data fabrication and, or falsification, double publication and, or submission, and redundancy have been completely witnessed by the authors.

Acknowledgment

We would like to express our gratitude to the editors and reviewers of JECEI for their valuable feedback and support during the review process. This work was entirely self-supported, with no financial support from any external agency.

Funding

This research received no external funding.

Abbreviations

BEMF	Back-Electromotive Force

EV	Electric Vehicle
FEA	Finite Element Analysis
FOC	Field-Oriented Control
IPMSM	Interior Permanent Magnet Synchronous Motor
MMF	Magneto Motive Force
MOPSO	Multi Objective Particle Swarm Optimization
PSO	Particle Swarm Optimization
SO-DT-IPMSM	Stator-Optimized Delta-Type Interior Permanent Magnet Synchronous Motor
SPMSM	Surface-mounted Permanent Magnet Synchronous Motor
THD	Total Harmonic Distortion

References

[1] X. Zhao, B. Kou, C. Huang, L. Zhang, "A reverse-salient permanent magnet synchronous motor for electric vehicles considering operating conditions," IEEE Trans. Energy Convers., 38(1): 262–272, 2023.

[2] Y. Xu, M. Ai, Z. Xu, W. Liu, Y. Wang, "Research on interior permanent magnet synchronous motor based on performance matching of electric bus," IEEE Trans. Appl. Supercond., 31(8): 5204304, 2021.

[3] J. Liu, Y. Liang, P. Yang, "Research on novel flat wire transposed winding of PMSM for electric vehicle," IEEE Trans. Transp. Electrif., 9(1): 771–781, 2023.

[4] J. Pyrhönen, T. Jokinen, V. Hrabovcová, Design of Rotating Electrical Machines, vol. I. New York: Wiley, 2013.

[5] Y. Wang, N. Bianchi, R. Qu, "Comparative study of non-rare-earth and rare-earth PM motors for EV applications," Energies, 15(7): 2711, 2022.

[6] L. Wang, X. Wang, P. Gao, "Torque ripple reduction analysis of interior permanent magnet synchronous motor for electric vehicle," Trans. China Electrotech. Soc., 39(20): 6386–6396, 2024.

[7] T. Gundogdu, G. Komurgoz, "A systematic design optimization approach for interior permanent magnet machines equipped with novel semi-overlapping windings," Struct. Multidiscip. Optim., 63(3): 1491–1512, 2021.

[8] J. Liang, A. Parsapour, Z. Yang, C. Caicedo-Narvaez, M. Moallem, B. Fahimi, "Optimization of air-gap profile in interior permanent-magnet synchronous motors for torque ripple mitigation," IEEE Trans. Transp. Electrif., 5(1): 118–125, 2019.

[9] G. Zhang, W. Yu, W. Hua, R. Cao, H. Qiu, A. Guo, "The design and optimization of an interior permanent magnet synchronous machine applied in an electric traction vehicle requiring a low torque ripple," Appl. Sci., 9(17): 3634, 2019.

[10] Y. Xu, Y. Chen, Z. Fu, M. Xu, H. Liu, L. Cheng, "Design and analysis of an interior permanent magnet synchronous motor for a traction drive using multi-objective optimization," Int. Trans. Electr. Energy Syst., 2024: 1–15, 2024.

[11] S. Lim, S. Min, J. P. Hong, "Shape design optimization of interior permanent magnet motor for vibration mitigation using level set method," Int. J. Automot. Technol., 17: 917–922, 2016.

[12] X. Sun, Z. Shi, G. Lei, Y. Guo, J. Zhu, "Multi-objective design optimization of an IPMSM based on multilevel strategy," IEEE Trans. Ind. Electron., 68(1): 139–148, 2021.

[13] X. Zhu, J. Huang, L. Quan, Z. Xiang, B. Shi, "Comprehensive sensitivity analysis and multi-objective optimization research of permanent magnet flux-intensifying motors," IEEE Trans. Ind. Electron., 66(4): 2613–2627, 2019.

[14] Y. Yu, Y. Pan, Q. Chen, Y. Hu, J. Gao, Z. Zhao, S. Niu, S. Zhou, "Multi-objective optimization strategy for permanent magnet synchronous motor based on combined surrogate model and optimization algorithm," Energies, 16: 1630, 2023.

[15] G. Feng, C. Lai, N. C. Kar, "Practical testing solutions to optimal stator harmonic current design for PMSM torque ripple minimization using speed harmonics," IEEE Trans. Power Electron., 33: 5181–5191, 2018.

[16] F. Xiong, R. Yan, Y. Xie, K. Yang, "Design and optimization of an interior permanent-magnet synchronous motor for aircraft drive application," Appl. Sci., 14: 309, 2024.

[17] Y. Yu, C. Liang, D. Zeng, Y. Hu, J. Yang, "Multi-objective optimization of IPMSM for electric vehicles based on the combinatorial surrogate model and the hierarchical design method," Int. J. Electr. Power Energy Syst., 162: 110245, 2024.

[18] K. S. Seo, Y. J. Kim, S. Y. Jung, "Stator teeth shape design for torque ripple reduction in surface-mounted permanent magnet synchronous motor," in Proc. 2014 17th International Conference on Electrical Machines and Systems (ICEMS): 387–390, 2014.

[19] L. Niu, "Optimization design and torque performance research of interior permanent magnet synchronous motors," Sci. Rep., 15: 8822, 2025.

[20] X. Kong, Z. Yang, "Multi-objective optimization of dual-stator permanent magnet motor based on composite algorithm," Sci. Rep., 15: 22982, 2025.

[21] X. Zhou, X. Zhu, W. Wu, Z. Xiang, Y. Liu, L. Quan, "Multi-objective optimization design of variable-saliency-ratio PM motor considering driving cycles," IEEE Trans. Ind. Electron., 68(8): 6516–6526, 2021.

[22] J. M. Ahn, M. K. Baek, S. H. Park, D. K. Lim, "Optimal design of IPMSM for EV using subdivided Kriging multi-objective optimization," Processes, 9(9): 1490, 2021.

[23] R. Yang, Electrified Vehicle Traction Machine Design with Manufacturing Considerations, Ph.D. dissertation, Dept. Mechanical Eng., McMaster Univ., Hamilton, ON, Canada, 2017.

[24] Y. Inoue, Y. Kawaguchi, S. Morimoto, M. Sanada, "Performance improvement of sensorless IPMSM drives in a low-speed region using online parameter identification," IEEE Trans. Ind. Appl., 47(2): 798–804, 2011.

[25] W. Feng, W. Zhang, S. Huang, "A novel parameter estimation method for PMSM by using chaotic particle swarm optimization with dynamic self-optimization," IEEE Trans. Veh. Technol., 72(7): 8424–8432, 2023.

[26] S. Zheng, X. Zhu, L. Xu, "Multi-objective optimization design of a multi-permanent-magnet motor considering magnet characteristic variation effects," IEEE Trans. Ind. Electron., 69: 3428–3438, 2022.

[27] P. P. C. Bhagubai, J. G. Sarrico, J. F. P. Fernandes, P. J. Costa Branco, "Design, multi-objective optimization, and prototyping of a 20 kW 8000 rpm permanent magnet synchronous motor for a competition electric vehicle," Energies, 13: 2465, 2020.

[28] M. Mendizabal, A. McCloskey, J. Poza, S. Zarate, L. Irazu, "Sensitivity analysis of the design parameters of permanent magnet synchronous motors for vibration reduction," Appl. Sci., 13: 5486, 2023.

[29] Y. Wang, M. Zhao, X. Jia, et al., "Analysis and multi-objective optimization of an interior permanent magnet synchronous

motor for a comprehensive performance enhancement," Struct. Multidiscip. Optim., 68: 55, 2025.

[30] S. Zhang, H. Yan, L. Yang, H. Zhao, X. Du, J. Zhang, "Optimization design of permanent magnet synchronous motor based on multi-objective artificial hummingbird algorithm," Actuators, 13: 243, 2024.

[31] S. Ahmadi, T. Lubin, A. Vahedi, N. Taghavi, "Sensitivity-based optimization of interior permanent magnet synchronous motor for torque characteristic enhancement," Energies, 14: 2240, 2021.

[32] X. Li, G. Li, Z. Han, X. Han, "High-torque and low-noise IPMSM multi-objective collaborative optimization based on multi-layer surrogate model," Authorea, 2024.

[33] H. Chen, C. H. T. Lee, "Parametric sensitivity analysis and design optimization of an interior permanent magnet synchronous motor," IEEE Access, 7: 159918–159929, 2019.

[34] X. Luo, G. Liu, B. Xie, L. Zhu, F. Zhang, "Review of sensitivity analysis methods for optimal design parameters of motors," Chin. J. Electr. Eng., 11: 114–135, 2025.

[35] F. Liu, X. Wang, H. Wei, "Electromagnetic performance analysis, prediction, and multi-objective optimization for U-type IPMSM," IEEE Trans. Ind. Electron., 71(9): 10322–10334, 2024.

[36] Y. Yu, P. Zhao, Y. Hao, D. Zeng, Y. Hu, B. Zhang, H. Yang, "Multi-objective optimization of permanent magnet synchronous motor based on Taguchi method and PSO algorithm," Energies, 16: 267, 2022.

[37] S. Nasr, B. Ganji, M. Moallem, "Design optimization of the delta-shape interior permanent magnet synchronous motor for electric vehicle application," J. Electr. Comput. Eng. Innovations (JECEI), 11: 291–300, 2023.

Biographies

Alireza Shams was born in Isfahan, Iran, in 1995. He received B.Sc. degree in Electrical Engineering from Technical and Vocational University, in 2018 and M.Sc. degree in Electrical Engineering from Malek-Ashtar University of Technology, Isfahan, Iran, in 2020. He is currently pursuing the Ph.D. degree in power electronics and electrical machines with Lorestan University, Khoramabad, Iran. His research interests include electric vehicle propulsion systems, IPMSM design optimization, torque ripple minimization, and efficiency improvement.

- Email: alireza.sh.esf.74@gmail.com
- ORCID: 0009-0000-5247-1398
- Web of Science Researcher ID: NA
- Scopus Author ID: NA
- Homepage: NA

Esmaeel Rokrok was born in Khoramabad, Iran, in 1972. He received his B.S., M.S. and Ph.D. degrees in Electrical Engineering from the Isfahan University of Technology, Isfahan, Iran, in 1985, 1997 and 2010, respectively. He is presently working as an Assistant Professor in the Department of Electrical Engineering, Lorestan University, Khoramabad, Iran. His current research interests include power system control and dynamics, dispersed generation, microgrids, power electronics and robust control.

- Email: rokrok.e@lu.ac.ir
- ORCID: 0000-0002-5034-4659
- Web of Science Researcher ID: NA
- Scopus Author ID: NA
- Homepage: https://professors.lu.ac.ir/show/?id=245

Behrooz Rezaeealam received the B.S. degree from Isfahan University of Technology in 1997, the M.S. and Ph.D. degrees from University of Tehran in 2000 and 2005, respectively, all in electrical engineering. He is currently an associate professor in the department of electrical engineering, Lorestan University, Iran. His research interests include modeling and design using FEM, electrical machines and drives.

- Email: rezaee.bh@lu.ac.ir
- ORCID: 0000-0002-9391-4826
- Web of Science Researcher ID: NA
- Scopus Author ID: NA
- Homepage: https://professors.lu.ac.ir/show/?id=240

Abbas-Ali Zamani was born in 1986 in Isfahan, Iran. He earned a B.Sc. degree in electronic engineering from Hakim Sabzevari University in Iran in 2009, and an M.Sc. degree in control engineering from Isfahan University of Technology in 2011. In 2018, he received his Ph.D. in control engineering from the University of Sistan and Baluchestan in Iran. Dr. Zamani is currently an assistant professor in the Department of Electrical Engineering, Technical and Vocational University, Iran. Seismic control, power system control, smart grids, renewable energies, and artificial intelligence are among his research interests.

- Email: a-zamani@tvu.ac.ir
- ORCID: 0000-0002-3654-7767
- Web of Science Researcher ID: NA
- Scopus Author ID: NA
- Homepage: https://profs.tvu.ac.ir/fa/teacher_db/179192